

Mechanism of the hydrophobic effect in the biomolecular recognition of arylsulfonamides by carbonic anhydrase

Phillip W. Snyder^a, Jasmin Mecinović^a, Demetri T. Moustakas^a, Samuel W. Thomas III^a, Michael Harder^a, Eric T. Mack^a, Matthew R. Lockett^a, Annie Héroux^b, Woody Sherman^c, and George M. Whitesides^{a,d,1}

^aDepartment of Chemistry and Chemical Biology, Harvard University, 12 Oxford Street, Cambridge, MA 02138; ^bNational Synchrotron Light Source, Brookhaven National Laboratory, 725 Brookhaven Avenue, Upton, NY 11973-5000; ^cSchrödinger, Inc., 120 West 45th Street, New York, NY 10036-4041; and ^dWyss Institute of Biologically Inspired Engineering, Harvard University, 60 Oxford Street, Cambridge, MA 02138

Contributed by George M. Whitesides, August 27, 2011 (sent for review June 16, 2011)

The hydrophobic effect—a rationalization of the insolubility of nonpolar molecules in water—is centrally important to biomolecular recognition. Despite extensive research devoted to the hydrophobic effect, its molecular mechanisms remain controversial, and there are still no reliably predictive models for its role in protein–ligand binding. Here we describe a particularly well-defined system of protein and ligands—carbonic anhydrase and a series of structurally homologous heterocyclic aromatic sulfonamides—that we use to characterize hydrophobic interactions thermodynamically and structurally. In binding to this structurally rigid protein, a set of ligands (also defined to be structurally rigid) shows the expected gain in binding free energy as hydrophobic surface area is added. Isothermal titration calorimetry demonstrates that enthalpy determines these increases in binding affinity, and that changes in the heat capacity of binding are negative. X-ray crystallography and molecular dynamics simulations are compatible with the proposal that the differences in binding between the homologous ligands stem from changes in the number and organization of water molecules localized in the active site in the bound complexes, rather than (or perhaps in addition to) release of structured water from the apposed hydrophobic surfaces. These results support the hypothesis that structured water molecules—including both the molecules of water displaced by the ligands and those reorganized upon ligand binding—determine the thermodynamics of binding of these ligands at the active site of the protein. Hydrophobic effects in various contexts have different structural and thermodynamic origins, although all may be manifestations of the differences in characteristics of bulk water and water close to hydrophobic surfaces.

physical-organic | entropy | surface water | benzo-extension | hydration

The hydrophobic effect—the energetically favorable association of nonpolar surfaces in an aqueous solution—often dominates the free energy of binding of proteins and ligands (1–5). Frequently, increasing the nonpolar surface area of a ligand decreases its dissociation constant (K_d ; i.e., increases the strength of binding) (6), and simultaneously decreases its equilibrium constant for partitioning from a hydrophobic phase to aqueous solution (K_p) (7). Modern, structure-guided, ligand design has relied upon the “lock-and-key” notion of conformational association between the atoms of the ligand and the binding pocket of a protein; the detailed molecular basis for the hydrophobic effect, however, continues to be poorly understood (1–5). This lack of understanding of the hydrophobic effect prevents accurate prediction of the free energy of binding of proteins and ligands.

The first, and currently most pervasive, rationale for the hydrophobic effect was based on studies of the thermodynamics of partitioning of nonpolar solutes from hydrophobic phases (i.e., the gas phase or a hydrophobic liquid phase) into water. The thermodynamics of partitioning of solute molecules is characterized by a dominant, unfavorable entropy and an increase in heat capacity of the aqueous system (8). The classical mechanism for

hydrophobicity, proposed by Frank and advanced by Kauzmann, Tanford, and many others, predicted that water near nonpolar solutes was more “ordered” than bulk water (1–5, 8–10). This so-called “iceberg” model rationalized thermodynamic parameters for partitioning at room temperature, and were compatible with both calorimetric studies of the solvation of small molecules and with structural studies of the methane clathrate-hydrates (11, 12). Although modeling studies have supported the classical mechanism (13, 14), neutron scattering experiments designed specifically to probe the structure of water have failed to observe such order near nonpolar solutes (15, 16).

Alternative theoretical approaches for modeling the hydrophobic effect—including those based on scaled-particle theory and its intellectual progeny (17–20)—also rationalize the unfavorable entropic component of transferring nonpolar molecules from a hydrophobic phase to an aqueous phase. These theories propose that the accumulation of “void volume” sufficient to accommodate a nonpolar solute in water is entropically unfavorable. Although these void volume theories have been criticized because they do not rationalize the heat capacities of partitioning (1), they do predict a size-dependence of the thermodynamics of water near nonpolar solutes: Small solutes (less than approximately 1 nm in diameter, similar in size to the nonpolar gases studied by Frank) fit into the hydrogen bonded network of liquid water without breaking hydrogen bonds, but the solvation of larger solutes requires water to sacrifice hydrogen bonds to maintain van der Waals contact with the solute. Water near solutes with diameters greater than approximately 1 nm, in the void volume models, have a structure that is enthalpically less favorable than that of bulk water (2). A body of spectroscopy studies support the prediction that molecules of water near extended hydrophobic surfaces participate in fewer hydrogen bonds than do molecules of bulk water (21, 22).

The prediction that the thermodynamics of water near solutes depends on the size—and implicitly on the shape—of the solute has influenced modern models of the hydrophobic effect. In particular, the inhomogeneous solvation theory of Lazaridis predicts that water in chemically heterogeneous cavities (like those that characterize the binding pockets of many proteins) possess structures that have free energies less favorable than the structure

Author contributions: P.W.S. and G.M.W. designed research; P.W.S., J.M., D.T.M., S.W.T., M.H., E.T.M., M.R.L., A.H., and W.S. performed research; P.W.S., J.M., D.T.M., S.W.T., M.H., A.H., and W.S. analyzed data; and P.W.S., W.S., and G.M.W. wrote the paper.

The authors declare no conflict of interest.

Data deposition: The crystallography, atomic coordinates, and structure factors have been deposited in the Protein Data Bank, www.pdb.org (PDB ID codes 3575, 3571, 3578, 3574, 3577, 3573, 3576, and 3572).

¹To whom correspondence should be addressed. E-mail: gwhitesides@gmwgroup.harvard.edu.

This article contains supporting information online at www.pnas.org/lookup/suppl/doi:10.1073/pnas.1114107108/-DCSupplemental.

We chose the buffer phase as a reference state and calculated the free energy, enthalpy, and entropy of the benzo group in octanol and in the binding pocket of HCA (Fig. 2B). This calculation indicates that: (i) solvation of the benzo group in aqueous buffer is roughly $+2 \text{ kcal mol}^{-1}$ higher (less favorable) in free energy than it is either in solution, in octanol, or in association with the binding pocket of HCA; (ii) association of the benzo group with the binding pocket is roughly -3 kcal mol^{-1} more favorable in enthalpy than solvation of that group in octanol; and (iii) association of the benzo group with the binding pocket is $+3 \text{ kcal mol}^{-1}$ less favorable in entropy than solvation of that group in octanol. Entropy and enthalpy, thus, compensate in the transfer of the benzo substituent from nonpolar solvent to the binding pocket, with binding of the hydrophobic group being characterized by a favorable enthalpic term.

To rationalize these results, we used X-ray crystallography to characterize each of the eight HCA–ligand complexes; the resolution of these structures was in the range of 1.25–1.97 Å (Table S4). The average root-mean-squared deviation of the alignment of the heavy atoms of the proteins was $0.15 \pm 0.04 \text{ Å}$, and that of all residues having at least one atom within 5 Å of atoms of the ligand was $0.10 \pm 0.02 \text{ Å}$ (Fig. 3A). The crystal structures also indicated that each of the ligands bind to HCA with the same geometry (Fig. 3B). We inferred from the structural data that the thermodynamics of binding are not due to changes in the crystallographically determined structure of the protein on binding the ligands, or due to differences between the geometry of the Zn^{II} -N bond of the monocyclic and bicyclic ligands.

The structural data also indicate that the atoms of the fused benzo ring make few contacts with residues in the hydrophobic shelf (Fig. 3C): The fused rings are in contact with three nonpolar residues from the hydrophobic shelf (Phe 131, Pro 202, and Leu 198), and with two polar groups (the hydroxyl of Thr 200 and the carbonyl oxygen of Pro 201). Remarkably, the hydropho-

bic effect, in this system, thus does not involve extensive contact of the apposed hydrophobic surfaces of protein and ligand. Of the three nonpolar contacts, only two (Phe 131 and Pro 202) differentiate the benzo ring from the five-membered ring. There is, therefore, a net increase of only two additional hydrophobic contacts (approximately 90 Å^2) upon the addition of the fused benzo ring. One face of the benzo ring, thus, forms a cavity, which has a volume of 50 Å^3 , with residues Phe 131 and Pro 202 of the hydrophobic wall: The value of $\Delta\Delta G^{\circ}_{\text{unbind,benzo}}$, in this case, is not the result of conformational association of the “lock” and the “key.”

Values of $\Delta C^{\circ}_{p,\text{bind}}$ for two ligands (T and BT) over the temperature range of 283–303 K (Fig. 4A) are negative ($\Delta C^{\circ}_{p,\text{bind}} = -38 \pm 7 \text{ cal mol}^{-1} \text{ K}^{-1}$ for T, and $-96 \pm 6 \text{ cal mol}^{-1} \text{ K}^{-1}$ for BT); these values indicate the involvement of solvent in determining the thermodynamics of binding (3, 5, 36). Calorimetric studies that correlate values of ΔC°_p of unfolding to the difference in surface area between the folded and unfolded states of numerous proteins predict a contribution of $-0.28 - 0.51 \text{ cal mol}^{-1} \text{ K}^{-1} \text{ Å}^{-2}$ of buried nonpolar surface area, and a contribution of $+0.14 - 0.26 \text{ cal mol}^{-1} \text{ K}^{-1} \text{ Å}^{-2}$ of buried polar surface area (43). Our estimate of $\Delta\Delta C^{\circ}_{p,\text{bind}} = -58 \pm 9 \text{ cal mol}^{-1} \text{ K}^{-1}$ is, thus, approximately twice that predicted from the crystal structures for the burial of surface area alone ($\Delta\Delta C^{\circ}_{p,\text{predicted}} = -30 \pm 5 \text{ cal mol}^{-1} \text{ K}^{-1}$).

Changes in heat capacity, however, also occur with the ordering of water molecules in protein–ligand complexes (29, 39). Connolly has estimated a maximum value of $-9 \text{ cal mol}^{-1} \text{ K}^{-1}$ for the ordering of one water molecule in a protein–ligand complex (42). Our thermochemical data, thus, are consistent with the ordering of two to four additional water molecules in the HCA–bicyclic ligand complexes than are ordered in the structures of HCA–monocyclic ligand complexes.

Crystallography is compatible with the hypothesis that water in the binding pocket of HCA determines the hydrophobic effect in this system: In the structures of HCA with the bicyclic ligands, between three and five molecules of water appear ordered between the benzo group and the polar wall. Crystallography does not, however, allow us to examine molecules of water that are not localized. Also, we cannot correlate (based solely on the positions of the crystallographically observable molecules of water) the influence of the change in the structure of the network of water molecules and the thermodynamics of binding of the ligands.

To estimate the contribution from water to the free energy of binding, we used the WaterMap method (Schrödinger Inc.) to predict the positions, enthalpies, and entropies of the water molecules in the binding pockets of the complexes of HCA–T, HCA–BT, HCA–F, and HCA–BF (Fig. 4 and Table S5). These calculations use an explicit-solvent molecular dynamics simulation, followed by clustering of the water molecules into “hydration sites,” which are nonoverlapping spheres of 1.0 Å radius (46). WaterMap uses inhomogeneous solvation theory to estimate the enthalpy and entropy of each hydration site (23, 24). To estimate the enthalpy and entropy of hydration of each complex, we calculated the sum of the 30 hydration sites closest to the ligand; this group of sites occupied a volume extending over a distance of roughly 10 Å from the surface of the ligand. Beyond this distance, the water–water correlation diminishes to zero and the radial distribution function of the hydration sites approaches one (i.e., that of bulk water). Because the relevant thermodynamic parameters in our case were those of benzo-extension, we compared the hydration of each monocyclic-HCA complex to that of the bicyclic-HCA complex (e.g., $\Delta\Delta G^{\circ}_{\text{WM,benzo}} = \Delta G^{\circ}_{\text{BT}} - \Delta G^{\circ}_{\text{T}}$). Our rationale was that—independent of the absolute accuracies of any calculations—the positions and relative energies of the hydration sites would reflect changes to the local structure of water induced by benzo-extension.

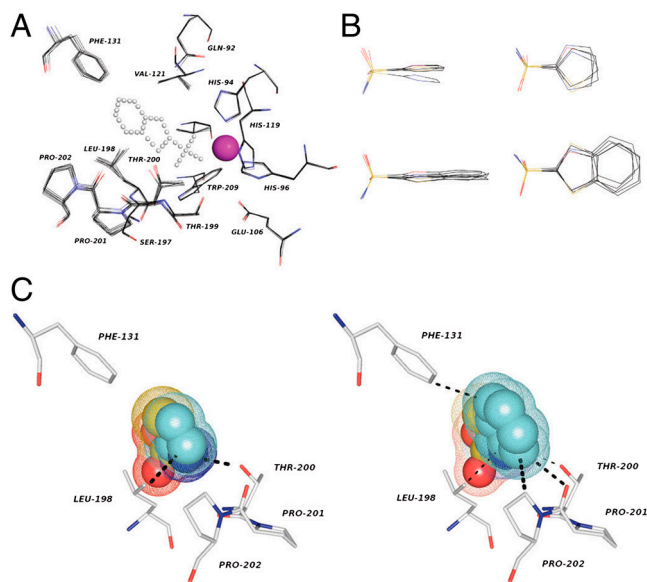


Fig. 3. Structural alignment of the eight available HCA–ligand complex structures F, BF, T, BT, I, BI, TA, and BTA. (A) Residues of the protein with atoms within 5 Å of the ligand in each structure appear as line diagrams. The magenta sphere indicates the position of the Zn^{II} ion. The white dashed lines indicate the position of the ligand. (B) Detailed view of all the heavy atoms of the sulfonamide ligands from the aligned HCA–ligand complex structures. (C) A representation of the contacts between the atoms of protein and the atoms of TA (Left) and BTA (Right). The atoms of the ligands appear as a space-filling representation; the green mesh represents the van der Waals contact surface. Dashed black lines indicate contacts between the ligands and the protein, and the radii of the lines are proportional to the interfacial contact area between the residue and the benzo substituent.

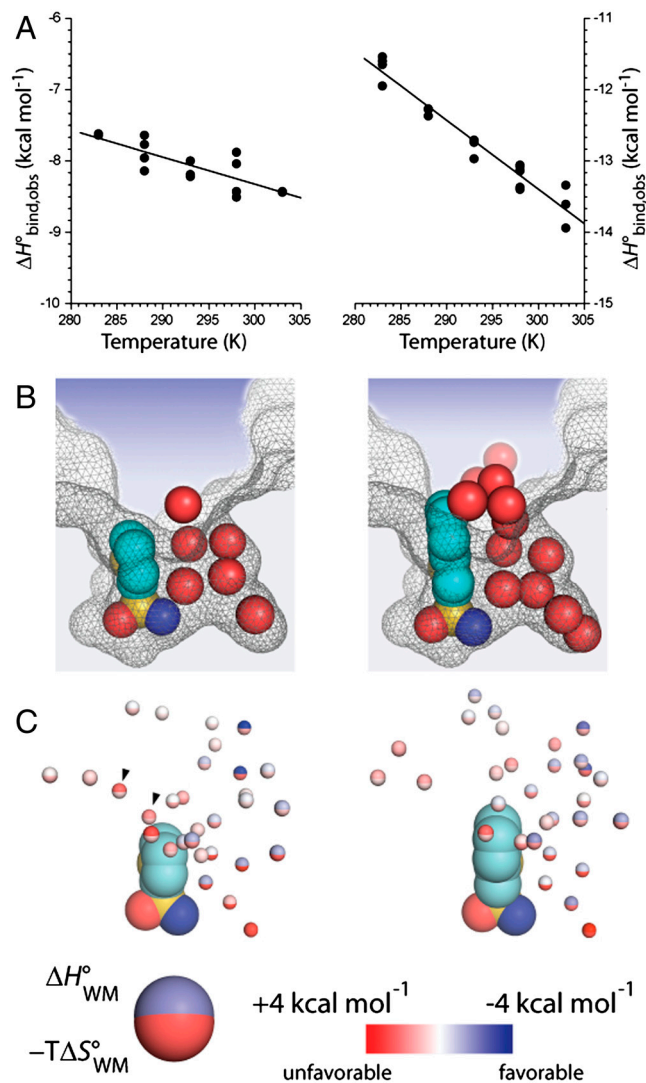


Fig. 4. (A) Observed enthalpies of binding as a function of temperature between 283 and 303 K. Enthalpy of binding was measured by ITC with independent titrations conducted at each temperature. Each datum represents a single ITC experiment. The black line indicates a linear fit of the data. The slope of the regression line was -38 ± 7 cal mol^{-1} K^{-1} for T, and was -96 ± 6 cal mol^{-1} K^{-1} for BT. (B) Positions of the molecules of water observed in the crystal structures of T and BT. The binding pocket of HCA appears as a mesh surface representation. Atoms of the ligands and crystallographically determined molecules of water appear as sphere representations. The corresponding images of six additional HCA–ligand complexes appear in *SI Text* (Fig. S3). (C) Results of the WaterMap calculations. The heavy atoms of the ligand appear as sphere representations (Left, T and Right, BT). The hydration sites from WaterMap appear as spheres that are color-coded to represent the predicted values of enthalpy and entropy: The top hemisphere represents enthalpy and the bottom hemisphere represents entropy. The color scale is set such that red represents hydration sites that are less favorable than bulk water, and blue represents those more favorable than bulk water.

Thermodynamic parameters calculated by WaterMap for benzo-extension were consistent with those determined experimentally by ITC (i.e., WaterMap also indicates that the gain in binding free energy comes from enthalpic stabilization). Average values for converting F to BF and T to BT were $\Delta\Delta G_{\text{WM,benzo}}^{\circ} = -2.8$ kcal mol^{-1} , $\Delta\Delta H_{\text{WM,benzo}}^{\circ} = -3.0$ kcal mol^{-1} , and $-T\Delta\Delta S_{\text{WM,benzo}}^{\circ} = 0.2$ kcal mol^{-1} (*SI Text* and *Table S5* detail the results of each calculation). The calculated values of entropy and enthalpy for each hydration site, moreover, provide some structural rationale for the enthalpically favorable hydrophobic effect. In particular, water molecules in two enthalpically unfa-

vorable hydration sites (indicated by arrows in Fig. 4C) in the binding pocket near the monocyclic ligand are displaced by benzo-extension. Additional changes to the network of water molecules in the binding pocket—including the ordering of water between the benzo group and the hydrophilic wall—result in entropy-enthalpy compensation, with the increased water ordering producing a loss in entropy. The cumulative effect of benzo-extension results in computed thermodynamic parameters that are indistinguishable from those determined experimentally by ITC. Although this agreement does not prove that changes in the water network are the origin of the hydrophobic effect in this system, it is compatible with that hypothesis.

An important conclusion from this work is that the phrase “hydrophobic effect” can have different molecular-level interpretations when it refers to partitioning of a ligand from a hydrophobic liquid phase to an aqueous phase, and from a hydrophobic binding pocket to the same aqueous phase. Thus, hydrophobic effects (plural) in biomolecular recognition and in partitioning between water and a nonpolar phase may have different structural and thermodynamic origins, although both may be manifestations of the differences in characteristics of water in bulk, and close to, surfaces. It thus appears that even for a given set of ligands, it is necessary to discuss multiple hydrophobic effects (with very different thermodynamic signatures) rather than a single hydrophobic effect: The tendency of nonpolar surfaces to associate reflects quite different balances of enthalpic and entropic effects, depending on molecular context, even though all (or many) may be manifestations of the structure of water.

Theoretical discussions by Rossky, Berne, Friesner, Lazaridis, and others (44–50, 53) have repeatedly suggested that the structure and thermodynamics of water adjacent to a nonpolar surface would depend on the molecular-scale topography of the surface. In this view, the difference in the structure and thermodynamics between water in the active site, and water in bulk, may determine the hydrophobic effect in the declivities that make up most binding pockets.

Although negative values of ΔC_p° are the sine qua non of hydrophobic interactions between proteins and ligands, the physical interpretation of this parameter remains as obscure as the experimental support for structured water near hydrophobic groups in dilute aqueous solution. We conclude that combined thermodynamic, biostructural, and computational studies of ΔC_p° of binding in systems of proteins and ligands continue to be necessary to untangle our understanding of hydrophobic effects. In that regard, HCA and arylsulfonamides seem to be an especially appropriate model system.

The combination of thermodynamic analysis, X-ray crystallography, and simulations described in this work is compatible with the hypothesis that the hydrophobic effect in biomolecular recognition, in this system, reflects changes in the structure of water extending across (and beyond) the active site region. The hydrophobic effect, here, cannot be attributed solely to the waters that are in contact with the nonpolar surfaces of the ligand, and it is not due to conformal association of the protein and ligand. In this view, the shape of the water in the binding cavity may be as important as the shape of the cavity.

Methods

SI Text details the experimental procedures for the purification of protein, the measurement of the thermodynamics of binding and partitioning, the measurement of the pK_a of the ligands, the preparation and crystallography of the protein–ligand complexes, and the calculation of the energies of the hydration sites for the HCA–ligand complexes.

ACKNOWLEDGMENTS. We thank Pat Connelly and Professor Eugene Shakhnovich for helpful discussions. This work was supported by the National Institutes of Health (NIH) (GM051559 and GM030367). Support for the National Synchrotron Light is provided by the US Department of Energy, and the NIH (P41RR012408).

1. Southall NT, Dill KA, Haymet ADJ (2002) A view of the hydrophobic effect. *J Phys Chem B* 106:521–533.
2. Chandler D (2005) Interfaces and the driving force of hydrophobic assembly. *Nature* 437:640–647.
3. Blokzijl W, Engberts JBFN (1993) Hydrophobic effects. Opinions and facts. *Angew Chem Int Edit* 32:1545–1579.
4. Meyer EA, Castellano RK, Diederich F (2003) Interactions with aromatic rings in chemical and biological recognition. *Angew Chem Int Edit* 42:1210–1250.
5. Ball P (2008) Water as an active constituent in cell biology. *Chem Rev* 108:74–108.
6. Houk KN, Leach AG, Kim SP, Zhang X (2003) Binding affinities of host–guest, protein–ligand, and protein–transition-state complexes. *Angew Chem Int Edit* 42:4872–4897.
7. Leo A, Hansch C, Elkins D (1971) Partition coefficients and their uses. *Chem Rev* 71:525–616.
8. Frank HS, Evans MW (1945) Free volume and entropy in condensed systems III. Entropy in binary liquid mixtures; partial molal entropy in dilute solutions; structure and thermodynamics in aqueous electrolytes. *J Chem Phys* 13:507–532.
9. Kauzmann W (1959) Some factors in the interpretation of protein denaturation. *Adv Protein Chem* 13:1–63.
10. Tanford C (1979) Interfacial free energy and the hydrophobic effect. *Proc Natl Acad Sci USA* 76:4175–4176.
11. Arnett EM, McKelvey DR (1969) Solvent isotope effect on thermodynamics of non-reacting solutes. *Solute–Solvent Interactions*, eds JF Coetzee and CD Ritchie (Dekker, New York).
12. Jeffrey GA (1969) Water structure in organic hydrates. *Acc Chem Res* 2:344–352.
13. Rossky PJ, Karplus M (1979) Solvation. A molecular dynamics study of a dipeptide in water. *J Am Chem Soc* 101:1913–1937.
14. Raschke TM, Levitt M (2005) Nonpolar solutes enhance water structure within hydration shells while reducing interactions between them. *Proc Natl Acad Sci USA* 6777–6782.
15. Turner J, Soper AK, Finney JL (1990) A neutron-diffraction study of tetramethylammonium chloride in aqueous solution. *Mol Phys* 70:679–700.
16. Buchanan P, Aldiwan N, Soper AK, Creek JL, Koh CA (2005) Decreased structure on dissolving methane in water. *Chem Phys Lett* 415:89–93.
17. Stillinger FH (1973) Structure in aqueous solutions of nonpolar solutes from the standpoint of scaled-particle theory. *J Solution Chem* 2:141–158.
18. Pratt LR, Chandler D (1977) Theory of the hydrophobic effect. *J Chem Phys* 67:3683–3705.
19. Lum K, Chandler D, Weeks JD (1999) Hydrophobicity at small and large length scales. *J Phys Chem B* 103:4570–4577.
20. Graziano G, Lee B (2003) Entropy convergence in hydrophobic hydration: A scaled particle theory analysis. *Biophys Chem* 105:241–250.
21. Richmond GL (2001) Structure and bonding of molecules at aqueous surfaces. *Annu Rev Phys Chem* 52:357–389.
22. Ji N, Ostroverkhov V, Tian CS, Shen YR (2008) Characterization of vibrational resonances of water-vapor interfaces by phase-sensitive sum-frequency spectroscopy. *Phys Rev Lett* 100:096102.
23. Lazaridis T (1998) Inhomogeneous fluid approach to solvation thermodynamics. 2. Applications to simple fluids. *J Phys Chem B* 102:3542–3550.
24. Lazaridis T (1998) Inhomogeneous fluid approach to solvation thermodynamics. 1. Theory. *J Phys Chem B* 102:3531–3541.
25. Lemieux RU (1996) How water provides the impetus for molecular recognition in aqueous solution. *Acc Chem Res* 29:373–380.
26. Williams BA, Chervenak MC, Toone EJ (1992) Energetics of lectin-carbohydrate binding. A microcalorimetric investigation of concanavalin A-oligomannoside complexation. *J Biol Chem* 267:22907–22911.
27. Chervenak MC, Toone EJ (1994) A direct measure of the contribution of solvent reorganization to the enthalpy of binding. *J Am Chem Soc* 116:10533–10539.
28. Ladbury JE, Wright JG, Sturtevant JM, Sigler PB (1994) A thermodynamic study of the trp repressor–operator interaction. *J Mol Biol* 238:669–681.
29. Clarke C, et al. (2001) Involvement of water in carbohydrate-protein binding. *J Am Chem Soc* 123:12238–12247.
30. Barratt E, et al. (2005) Van der Waals interactions dominate ligand–protein association in a protein binding site occluded from solvent water. *J Am Chem Soc* 127:11827–11834.
31. Malham R, et al. (2005) Strong solute-solute dispersive interactions in a protein–ligand complex. *J Am Chem Soc* 127:17061–17067.
32. Jencks WP (1969) *Catalysis in Chemistry and Enzymology* (McGraw-Hill, New York).
33. Salonen LM, Ellermann M, Diederich F (2011) Aromatic rings in chemical and biological recognition: Energetics and structures. *Angew Chem Int Edit* 50:4808–4842.
34. Homans SW (2007) Water, water everywhere—except where it matters? *Drug Discov Today* 12:534–539.
35. Mecinovic J, et al. (2011) Fluoroalkyl and alkyl chains have similar hydrophobicities in binding to the “hydrophobic wall” of carbonic anhydrase. *J Am Chem Soc* 133:14017–14026.
36. Oas TG, Toone EJ (1997) Thermodynamic solvent isotope effects and molecular hydrophobicity. *Adv Biophys Chem* 6:1–52.
37. Shimokhina N, Bronowska A, Homans SW (2006) Contribution of ligand desolvation to binding thermodynamics in a ligand–protein interaction. *Angew Chem* 118:6522–6524.
38. Bingham RJ, et al. (2004) Thermodynamics of binding of 2-methoxy-3-isopropylpyrazine and 2-methoxy-3-isobutylpyrazine to the major urinary protein. *J Am Chem Soc* 126:1675–1681.
39. Olsson TSG, Williams MA, Pitt WR, Ladbury JE (2008) The thermodynamics of protein–ligand interaction and solvation: Insights for ligand design. *J Mol Biol* 384:1002–1017.
40. Syme NR, Dennis C, Bronowska A, Paesen GC, Homans SW (2010) Comparison of entropic contributions to binding in a “hydrophilic” versus “hydrophobic” ligand–protein interaction. *J Am Chem Soc* 132:8682–8689.
41. Sturtevant JM (1977) Heat capacity and entropy changes in processes involving proteins. *Proc Natl Acad Sci USA* 74:2236–2240.
42. Connolly PR (1997) *Structure-Based Drug Design: Thermodynamics, Modeling and Strategy* (Springer, Berlin) p 188.
43. Prabhu NV, Sharp KA (2005) Heat capacity in proteins. *Annu Rev Phys Chem* 56:521–548.
44. Cheng Y-K, Rossky PJ (1998) Surface topography dependence of biomolecular hydrophobic hydration. *Nature* 392:696–699.
45. Liu P, Huang X, Zhou R, Berne BJ (2005) Observation of a dewetting transition in the collapse of the melittin tetramer. *Nature* 437:159–162.
46. Young T, Abel R, Kim B, Berne BJ, Friesner RA (2007) Motifs for molecular recognition exploiting hydrophobic enclosure in protein–ligand binding. *Proc Natl Acad Sci USA* 104:808–813.
47. Giovambattista N, Lopez CF, Rossky PJ, Debenedetti PG (2008) Hydrophobicity of protein surfaces: Separating geometry from chemistry. *Proc Natl Acad Sci USA* 105:2274–2279.
48. Beuming T, Farid R, Sherman W (2009) High-energy water sites determine peptide binding affinity and specificity of PDZ domains. *Protein Sci* 18:1609–1619.
49. Wang L, Berne BJ, Friesner RA (2011) Ligand binding to protein-binding pockets with wet and dry regions. *Proc Natl Acad Sci USA* 108:1326–1330.
50. Abel R, et al. (2011) Contribution of explicit solvent effects to the binding affinity of small-molecule inhibitors in blood coagulation factor serine proteases. *ChemMedChem* 6:1049–1066.
51. Freire E (2004) Isothermal titration calorimetry: Controlling binding forces in lead optimization. *Drug Discov Today Technol* 1:295–299.
52. Krishnamurthy VM, et al. (2008) Carbonic anhydrase as a model for biophysical and physical-organic studies of proteins and protein–ligand binding. *Chem Rev* 108:946–1051.
53. Setny P, Baron R, McCammon JA (2010) How can hydrophobic association be enthalpy driven? *J Chem Theory Comput* 6:2866–2871.